RELATIONSHIP OF MISR RPV PARAMETERS AND MODIS BRDF SHAPE INDICATORS TO SURFACE VEGETATION PATTERNS IN AN AUSTRALIAN TROPICAL SAVANNA

Michael J. Hill[1], Clare Averill[2], Ziti Jiao[3], Crystal B. Schaaf[3], John D. Armston[4]

Background

The global coverage of bi-directional reflectance distribution function (BRDF) products from the Multi-angle Imaging Spectroradiometer (MISR) and the Moderate Resolution Imaging Spectroradiometer (MODIS) could provide quantitative information on surface vegetation structure for input to process modelling and model-data assimilation schemes for regional and biome scale assessment of carbon dynamics. We examined the relationship of MISR RPV (Rahman-Pinty-Verstraete) model parameters, derived from inversion of MISR 275 m fine mode data, and BRDF shape indicators calculated from the latest MODIS 500 m MCD43 bidirectional reflectance distribution function (BRDF) product to vegetation patterns in an Australian tropical savanna, for a time series covering the dry season period from April to October 2005. The bi-directional reflectance products were compared with a GIS data coverage combining floristic polygons with Landsat TM-based estimates of canopy cover and height classes.

The RPV model and MISR

The Rahman-Pinty-Verstraete model (RPV) (Rahman et al., 1993) is a parametric model that describes the shape of the bidirectional reflectance distribution function. The model expresses the BRF $\rho(\Omega)$ as:

$\rho(\Omega) = \rho_0 F(\Omega; k, \Theta^{hg}, \rho_c)$

where $\rho 0$ is a parameter representing the amplitude of the BRF, and the function F characterizes the anisotropy of the landscape. The function $F(\Omega; k, \Theta^{hg}, \rho_c)$ requires the estimation of three parameters, k, Θ and ρ which are independent of illumination and observation geometry ($\Omega = \theta_i, \theta_v, \varphi$) and represent the status of the surfaces (Gobron et al., 2000).The main elements of the BRDF shape are separated into overall brightness (ρ_0), the bowl or bell shaped anisotropy (k), and the degree of forward or backward scattering (Θ). A modified version of the Rahman-Pinty-Verstrate model (MRPV) is used to provide RPV model parameters in the MISR Level 2 land surface product

The Ross-Thick Li-Sparse model and MODIS

The potential structural information provided by the MODIS BRDF product is derived from simplified linearized implementation of a surface anisotropy model – the Ross-thick Li-sparse Reciprocal model (RTLSR; Roujean et al., 1992; Wanner et al., 1995; Lucht et al., 2000). The RTLSR model is a semi-empirical BRDF model with geometric, isotropic and volume components (Roujean et al, 1992) parameterized from the physical turbid media models of Ross (1981) and the geometric-optical shadowing models of Li and Strahler (1992).

$$BRDF = f_{iso} + f_{vol} \times k_{vol}(\theta_i, \theta_v, \varphi) + f_{geo} \times k_{geo}(\theta_i, \theta_v, \varphi)$$

where k_{vol} is a function of view zenith θ_v and illumination zenith θ_i and describes the volume scattering from canopy and k_{geo} is a similar function that describes the shadowing and surface scattering from the canopy; φ is the relative azimuth between the solar and sensor directions.

The MODIS BRDF product is derived from this model and the linearized expansion of scattering terms can be used to create a range of geometric, isotropic and volumetric shape indicators that may be useful in describing vegetation structure (Gao et al., 2003; Table below).

Shape Indicator	Description
ANIF-Red; ANIF-NIR	Forward Scattering Anisotropy Index – Red and NIR; ratio of nadir to 45° forward scattering at 45° sun angle
ANIX-Red; ANIX-NIR	Backward Scattering Anisotropy Index - Red and NIR; ratio of 45° backward scattering to 45° degree forward scattering at 45° sun angle
NDHD-Red; NDHD-NIR	Normalised Difference Hotspot-Darkspot index – Red and NIR
AFX-Red; AFX-NIR	Ratio of white-sky albedo to BRDF isotropic parameter value – Red and NIR
NDAX	Normalised Difference Anisotropy Index at 45° sun angle; $NDAX = (ANIX_{sun} - ANIX_{sun})/(ANIX_{sun} + ANIX_{sun})$
SSI	Structural Scattering Index $SSI = \ln(\Gamma_{sun\,at\,0\,(nadir)})$

Code	Vegetation Description
A1	Mangroves
A3	Saline tidal mudflats +/- samphire
C21	*Eucalyptus microtheca* or *Eucalyptus gymnoteles* and/or *Eucalyptus* spp. +/- *Eucocaria parvifolia* grassy low woodland.
C28	*Melaleuca viridiflora* grassy low open-woodland +/- a shrub layer +/- emergent trees.
C35	Mixed species tussock grasslands or sedgelands +/- emergent *Pandanus* spp.and/or *Corypha utan*.
C41	*Melaleuca minutifolia* low woodland with *Sorghum* spp. tussock grasses.
C6	*Melaleuca* spp. open-forest.
D10	*Eucalyptus tectifica* and/or *Corymbia* spp. woodland with *Sorghum* spp.and *Sehima nervosum* tussock grasses.
D26	*Eucalyptus tetrodonta*
D3	*Eucalyptus miniata* and *Eucalyptus tetrodonta +/- Corymbia nesophila* open-forest with *Sorghum* spp. Tussock grasses.
D34	*Eucalyptus pruinosa +/- Lysiphyllum cunninghamii* low open-woodland +/- a shrub layer and tussock grasses or *Triodia* spp.
G19	*Dichanthium fecundum* and *Chrysopogon fallax* tussock grassland sparsely wooded with low trees.
H12	*Eucalyptus tetrodonta* and *Eucalyptus miniata +/- Corymbia bleeriwith Sorghum* spp. tall-grasses.
H18	*Eucalyptus phoenicea* and *Corymbia ferruginea* subsp. *stypophylla* low woodland with *Triodia bitextura* hummock grassland understorey.
H19	*Corymbia dichromophlota*
H2	Rainforest communities on sandstone
K12	*Eucalyptus miniata* grassy woodland.
K19	*Eucalyptus brevifolia* low open-woodland with *Triodia bitextura* hummock grass +/- *Enneapogon* spp. short-tussock grass or sometimes a grassland without trees.
K23	*Livistona humilis* grassy tall open-shrubland.

- Obtained MISR L1B2 Local Mode Terrain HDF-EOS files for three blocks in path 106 over the Howard Springs flux tower in the Northern Territory for 10 dates throughout the post-monsoonal season in 2005 – days 111, 127, 143, 158, 175, 191, 222, 235, 255 and 271.
- The local mode data were combined with L2AS_LAND and GMP layers to calculate surface bidirectional reflectance factors (BRFs) at 275m. (Armston et al., 2007).
- The local mode "at-sensor" L1B2 radiances were first converted to top of atmosphere (TOA) BRF and averaged to 1100m spatial resolution.
- Linear relationships were then established between the averaged local mode TOA BRF the MISR level 2 land surface BRFs using linear ordinary least squares (OLS) regression.
- The linear coefficients were then interpolated to 275m spatial resolution using bilinear interpolation and applied to the L1B2 275m TOA BRFs to calculate 275m surface BRFs.

Region and Vegetation

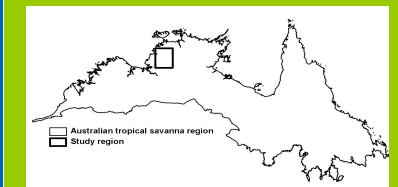

The Australian tropical savanna zone showing the location of the study region

Photos illustrating some of the specific vegetation types examined: a) Eucalypt-*Sorghum* woodland; b) Eucalypt-*Sehima* open woodland; c) *Melaleuca* shrub; d) *Dichanthium* grassland with scattered trees (Photos – M. J. Hill).

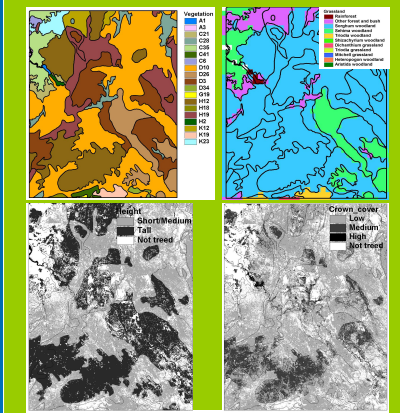

Top-left. Vegetation types. The legend code for vegetation corresponds to the listing in Table 2. Top-Right. Grassland understorey. Bottom-left. Tree canopy height. Bottom-right. Tree crown cover.

Vegetation was defined by local polygons based upon a combination of floristics (species classes), tree canopy cover and height classes. We then chose a sample of the floristic-structure types to illustrate the responses of MISR RPV parameters and MODIS BRDF shape indicators. These were chosen on the basis of: 1) distinct canopy structural differences, e.g., Eucalypt versus *Melaleuca* spp; 2) distinct canopy density and height differences, e.g., rainforest, Eucalypt/grass savanna with different canopy density and height classes; and 3) treed versus tree-less grassland, e.g., the Eucalypt savanna versus the *Dichanthium* sp. grassland. The types chosen varied in pixel counts from the most predominant cover types (7036 and 6952 pixels for *E. miniata* with grasses) down to small areas of the most different cover types (135, 163 and 290 pixels for *Melaleuca* spp. woodland (2) and *Dichanthium* sp. grasslands).

Armston, J. D., Scarth, P. F. Phinn, S. R., and Danaher, T. J. 2007. *Remote Sensing of Environment*, Vol. 107, pp. 287-298.
Chen, J. M., Menges C. H., and Leblanc, S. G. 2005. *Remote Sensing of Environment*, Vol. 97, pp. 447-457.
Gao, F., Schaaf, C. B., Strahler, A. H., Roesch, A., Lucht, W., and Dickinson, R. 2005. *Journal of Geophysical Research*, Vol. 110, D01104, doi:10.1029/2004JD005190.
Gobron, N., Pinty, B. Verstraete, M.M. Widlowski, J-L., and Diner D.J. 2002. *IEEE Transaction on Geoscience and Remote Sensing*, Vol. 40, pp. 1574-1592.
Li, X., and Strahler, A. H. 1992. *IEEE Transactions on Geoscience and Remote Sensing*, Vol. 30, pp. 276– 292.
Lucht, W., Schaaf, C. B., and Strahler, A. H. 2000. *IEEE Transactions on Geoscience and Remote Sensing*, Vol. 38, pp. 977-998.
Rahman, H., Verstraete, M. M. and Pinty B. (1993a). *Journal of Geophysical Research*, Vol. 98, pp. 20779-20789.
Ross, J. K. 1981. *The Radiation Regime and Architecture of Plant Stands*. Norwell, MA: Dr. W. Junk, 392 pp.
Roujean, J-L., Leroy, M., and Deschamps P-Y. 1992, *Journal of Geophysical Research*, Vol. 97, pp. 20455-20468.
Wanner, W., Li, X., and Strahler, A. H. 1995. *Journal of Geophysical Research*, D-100, 21077–21090.

Spatial Patterns and Temporal Dynamics

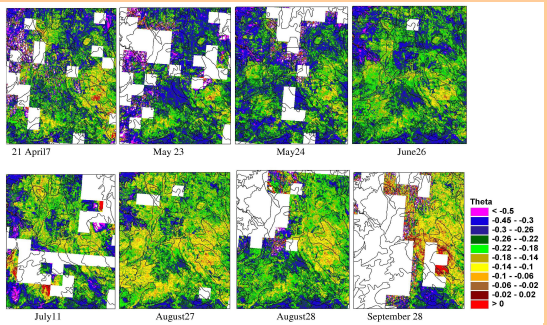

Time series of anisotropy (θ) parameter for the red band of MISR.

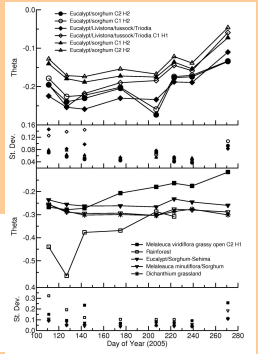

Temporal profiles of the anisotropy (θ) parameter from the RPV model for selected vegetation floristic and structural types in the savanna study region.

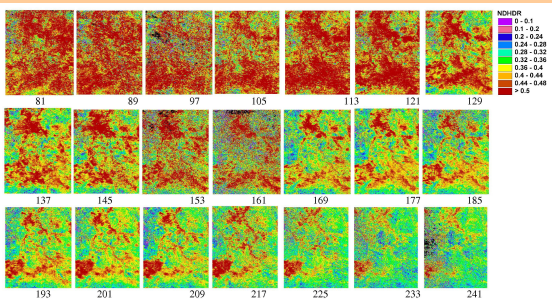

Time series of NDHD-R from day 81 to day 241 in 2005 over the Australia tropical savanna site near Darwin

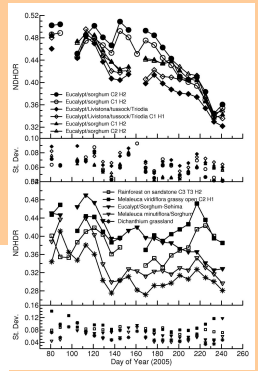

Temporal profiles of the NDHD-R shape indicator for selected vegetation floristic and structural types in the savanna study region.

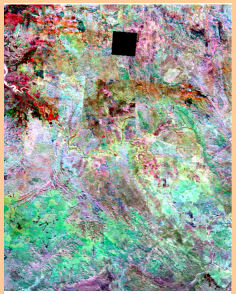

RGB images of MISR RPV θ (anisotropy) parameter for 24 June 2005. Red – NIR channel; green – red channel; blue – green channel. Image shows highly detailed spatial patterns related to small and subtle variations in the anisotropic scattering between NIR, red and green spectral bands.

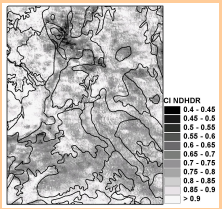

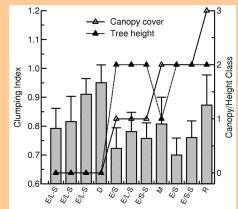

- We applied the regression coefficients for a SZA of 47.5 degrees from a half ellipsoid canopy model (Chen et al., 2005) to the NDHD-R image data to calculate a clumping index for day 177
- The resulting clumping index shows a strong resemblance to the pattern the canopy cover layer.
- Clumping increases as the value of the index decreases:
  - high values represent the very open savanna areas, predominantly grassland;
  - lower values correspond to woodland situations with a much higher tree canopy cover.
- When estimated clumping index is plotted for the main vegetation types:
  - higher values are associated with the most uniform canopies, *Dichanthium* grassland and rainforest;
  - there is significant variation among savanna types with canopy cover between 21 and 80%.
- Explanation requires more detailed understanding of the influence of different leaf types and orientations (e.g., different species of eucalypt, and *Melaleuca*), different individual tree canopy shapes and densities (e.g., "pom-pom" versus elliptical; sparse versus dense); and different arrangements of trees and open spaces (e.g., scattered versus clumped); and precise mapping of spatial arrangements provided by, for example, LiDAR.

Conclusions

The results from this work show that there may be significant and complimentary information about savanna vegetation structure within the high level BRDF products from both the MODIS and MISR sensors. Whilst a definitive relationship between savanna tree densities, arrangements, canopy shapes and tree heights could not be obtained with such broad descriptive structure classes, the results showed distinct differences between individual, spatially defined savanna communities, and considerable evidence of trends related to the aspect-ratio effects of canopy cover and tree height. We surmise that shadow casting, and arrangements of open space and tree clumps could be quantitatively characterised, and generalised to the scale of MISR and MODIS pixels. In order to do this, more detailed and quantitative vegetation descriptions than were available for this study are needed relate the structural information content of these products to actual three dimensional metrics of the "voxels" for MISR and MODIS pixels.

[1]**M. J. Hill** Earth System Science and Policy, University of North Dakota, Clifford Hall, Stop 9011, Grand Forks, North Dakota, 58202, USA.
[2]**C. Averill** NASA-JPL, MISR Team via Raytheon Information Solutions, Science Systems & Analysis, c/o Raytheon Australia
[3]**Z. Jiao and C. B. Schaaf** Department of Geography and Center for Remote Sensing, Boston University, 575 Commonwealth Avenue, Boston, MA 02215, USA
[4]**J. D. Armston** Remote Sensing Centre, Natural Resource Sciences, Queensland Department of Natural Resources and Water, 80 Meiers Road, Indooroopilly, Queensland, 4068, Australia